Journal of Renewable Energies

Revue des Energies Renouvelables

Journal home page: https://revue.cder.dz/index.php/rer

Research paper

Non-fullerene OSC: The effects of active and electron transport layers' thickness towards 19.5% efficiency

Burak Yahya Kadem [a], **R.K. Fakher Alfahed** [b,*]

[a] *College of Science, Al-Karkh University of Science, Baghdad, Iraq*

[b] *Al-Nahrain University, Al-Nahrain Renewable Energy Research Center, Jadriya, Baghdad, Iraq*

ARTICLE INFO	ABSTRACT
	The effects of the active layer thickness of the organic solar cells based on PM6, D18 and L8-BO materials as well as the effects of electron transport layer thickness are examined using Organic and hybrid Material Nano Simulation (Oghma) software. Several active layer thicknesses are used starting 50nm to 300nm to choose the optimum active layer thickness. For PM6:L8-BO blend, the optimum active layer thickness of is found to be 90nm with a PCE of 13.52%. Whereas, the optimum active layer thickness of D18:L8-BO blend is demonstrated almost similar characteristics with PCE of 13.2% for an optimum active layer thickness of 90nm. Using ternary blend PM6:D18:L8-BO active layer enhances the PCE to 17.5% when the optimum active layer thickness is 80nm. Also, the use of different electron transport layer thickness has resulted in further increase in the PCE to reach as high as 19.5% with the thickness of 20nm.

1. INTRODUCTION

Organic solar cells (OSCs) are considered as a promising technology due to their flexibility, light weight, low cost, and printability (Heeger, 2014). OSC flexibility is a unique characteristic compared with brittleness inorganic photovoltaic devices. Significant developments have been made during the last decade with power conversion efficiency (PCE) exceeding 19% in laboratory studies (He et al., 2022; Zheng et al., 2022). Typically, OSCs' architecture comprises of five layers: electron-transport layer (ETL), photoactive layer, hole-transport layer (HTL), and the two electrodes. Mainly, the photoactive and the interface layers have significant impact on the device performance, several studies have discussed these parameters in details (Bishnoi et al., 2022; Kadem et al., 2015; Yuan et al. 2019). For OSCs, it is essential to combine both organic materials (donor and acceptor) together in a bulk

heterojunction structure (BHJ). Such structure permits the separation of the strongly bounded Frenkel excitons via charge transfer to the other material and forming charge transfer (CT) states; the separation efficiency is correlated to the interface area between the two domains in the BHJ (Kadem et al., 2016). The development of OSC is limited by the relation between the generated voltage and current (Xue et al., (2018). Also, the energy difference between the highest occupied molecular orbital (HOMO) and lowest unoccupied molecular orbital (LUMO) of the absorbing materials has significant impact on altering the absorption properties and producing higher current. Where the generated voltage known as the open circuit voltage (VOC) is mainly determined by the difference between the HOMOdonor and the LUMOacceptor (Kadem et al., 2018). In the current study, organic and hybrid material nano simulation tool (Oghma) is used to simulate the organic solar cell (MacKenzie et al., 2016; Gao et al., 2016). Several parameters can be simulated in this program, however, we have focused on optimizing the best factors to achieve high device performance close to 20% efficiency. Binary and ternary blends are employed in this study and a comparison is made. As a donor material, Poly[(2,6-(4,8-bis(5-(2-ethylhexyl-3-fluoro) thiophen-2-yl) -benzo [1,2-b:4,5-b'] dithiophene))-alt- (5,5-(1',3'-di-2-thienyl-5', 7' -bis (2-ethylhexyl) benzo [1',2'-c:4',5'-c']dithiophene-4,8-dione)] known as (PM6) PBDB-T-2F is a PBDB-T family member is used. Using PM6 as the electron donor and Y6 as an electron acceptor in a single junction non-fullerene polymer solar cell results in certified efficiency of 14.9% (Yuan et al., 2019). Another electron donor, Poly[(2,6-(4,8-bis(5-(2-ethylhexyl-3-fluoro) thiophen-2-yl)- benzo [1,2-b:4,5-b'] dithiophene)) -alt-5,5'- (5,8-bis(4-(2-butyloctyl) thiophen-2-yl) dithieno [3',2':3,4;2'',3'':5,6] benzo[1,2-c][1,2,5]thiadiazole)] known as D18 is used. The latter is a narrow bandgap copolymer with a backbone alternating weaker electron-accepting unit known as DTBT and shares a key electron-donating unit, the fluorinated BDT. It has high hole mobility of $1.59 \times 10-3$ cm V−1 s−1. Organic solar cell based on D18:Y6 blend achieved a remarkable PCE of 18.22% (Sharma et al., 2023). Moreover, (2,2′- ((2Z,2′Z)- ((3,9-bis (2-butyloctyl) -12, 13-bis (2-ethylhexyl) -12,13-dihydro -[1,2,5]thiadiazolo[3,4-e]thieno[2′′,3′′:4′,5′] hieno [2′,3′:4,5] pyrrolo [3,2-g] thieno [2′,3′:4,5] thieno [3,2-b] indole-2,10-diyl) bis (methaneylylidene)) bis(5,6-difluoro-3-oxo-2,3-dihydro-1H-indene-2,1-diylidene))dimalononitrile) known as L8-BO is a non-fullerene acceptor is also used (Zhu et al., 2022). To achieve higher power conversion efficiency (PCE), the organic solar cell (OSC) structure should be optimized and the several parameters must take into account such as carrier diffusion length (Tokmoldin et al., 2021), bend structure (Lee, 2020), energy level alignments (Kadem et al., 2016), enhancing absorption properties (Kadem et al., 2019), electron and hole transport layers (Hassan et al., 2017). The device structure used in the current study is as follow: ITO/PEDOT:PSS (200nm)/ active layer/ PNDIT-F3N (10nm)/Ag. Different active layer thickness is used to achieve the optimum thickness with the higher PCE for each active layer in binary and ternary blends. Follow this, the best device with highest PCE is used to further investigate the effect of ETL with different thicknesses and choose the optimum thickness of ETL. Results are promising in fabrication non-fullerene OSC with PCE close to 20% with optimum active layer thickness of the ternary blend and the optimum ETL thickness. The device parameters used in this study is illustrated in Table 1.

To the best of the authors' knowledge, this study is the first to employ double non-fullerene acceptors with energy band alignments favourable for enhanced charge transfer and improved absorption properties, aiming to achieve higher power conversion efficiency in organic solar cells (OSCs). Several parameters were simulated to optimise the best parameters to achieve high device performance close to 20% efficiency**.**

Table 1. Device parameters used in the simulated solar cells

Active layer	D18:L8-BO	PM6:L8-BO	PM6:D18:L8-BO
Electron mobility ($m^2.V^{-1}. s^{-1}$)	1.4×10^{-7}	1.5×10^{-7}	1.49×10^{-7}
Hole mobility ($m^2.V^{-1}. s^{-1}$)	1.8×10^{-7}	1.15×10^{-7}	1.42×10^{-7}
Effective density of free electron states @300K (m^{-3})	1×10^{26}	1×10^{26}	1×10^{26}
Effective density of free hole states @300K (m^{-3})	1×10^{26}	1×10^{26}	1×10^{26}
Recombination rate ($m^3 s^{-1}$)	7.8×10^{-17}	1.77×10^{-17}	1.15×10^{-17}
Electron affinity (eV)	4.2	4.2	4.2
Relative permittivity	3	3	3
Band gap (eV)	1.32	1.28	1.29

2. RESULTS AND DISCUSSIONS

2.1 D18:L8-BO active layer

The simulated OSCs described in this section are based on using different active layer thicknesses of D18:L8-BO blend. The thickness plays a significant role in manipulating the device performance by affecting several parameters such as the exciton diffusion and enhancing photo-harvesting properties. To achieve efficient exciton generation rate and high charge transport and hence higher PCE, several active layer thicknesses of D18:L8-BO blend is used starting from 50nm to 300nm, where the exciton diffusion length of D18 material is about 24nm. (Zhu et al., 2022). Fig. 1A shows the J-V curves of the D18:L8-BO based OSCs with different active layer thicknesses. Results exhibited improvement in the solar cell characteristics with the optimum active layer thickness which is (90nm) compare to other thicknesses.
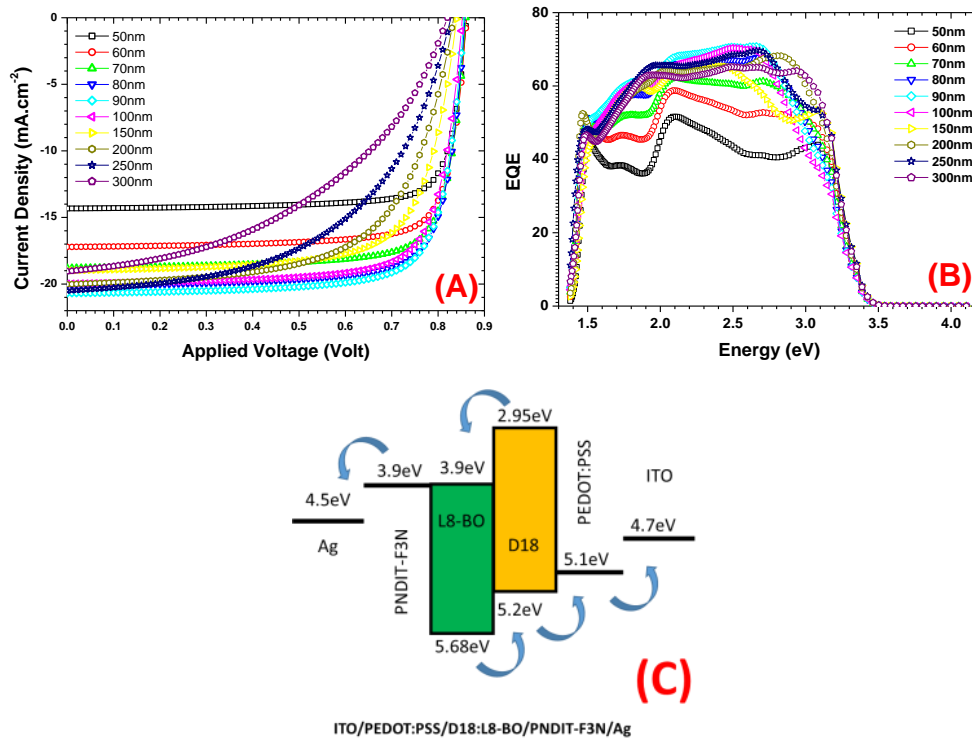

Fig 1. (A) J-V curves (B) EQE spectra and (C) Energy level alignments, of D18:L8-BO based OSCs

The EQE spectra of the OSCs shown in Fig. 1B revealed an enhancement in the photo harvesting characteristics by increasing the active layer thickness. D18 as a donor material can absorb photons in the wavelength range from 400 nm to 700 nm, whereas L8-BO as an acceptor material can broaden the absorption properties as it absorbs the photons in the wavelength range from 600nm to 900nm. Also, the energy level offset of D18 and L8-BO shown in Fig. 1C facilitates the charge carriers' extraction, dissociation and transportation between the donor and acceptor phases and this contributes in higher V_{OC} as it is mainly determined by the difference between the $HOMO_{donor}$ and the $LUMO_{acceptor}$ (Kadem et al., 2018).
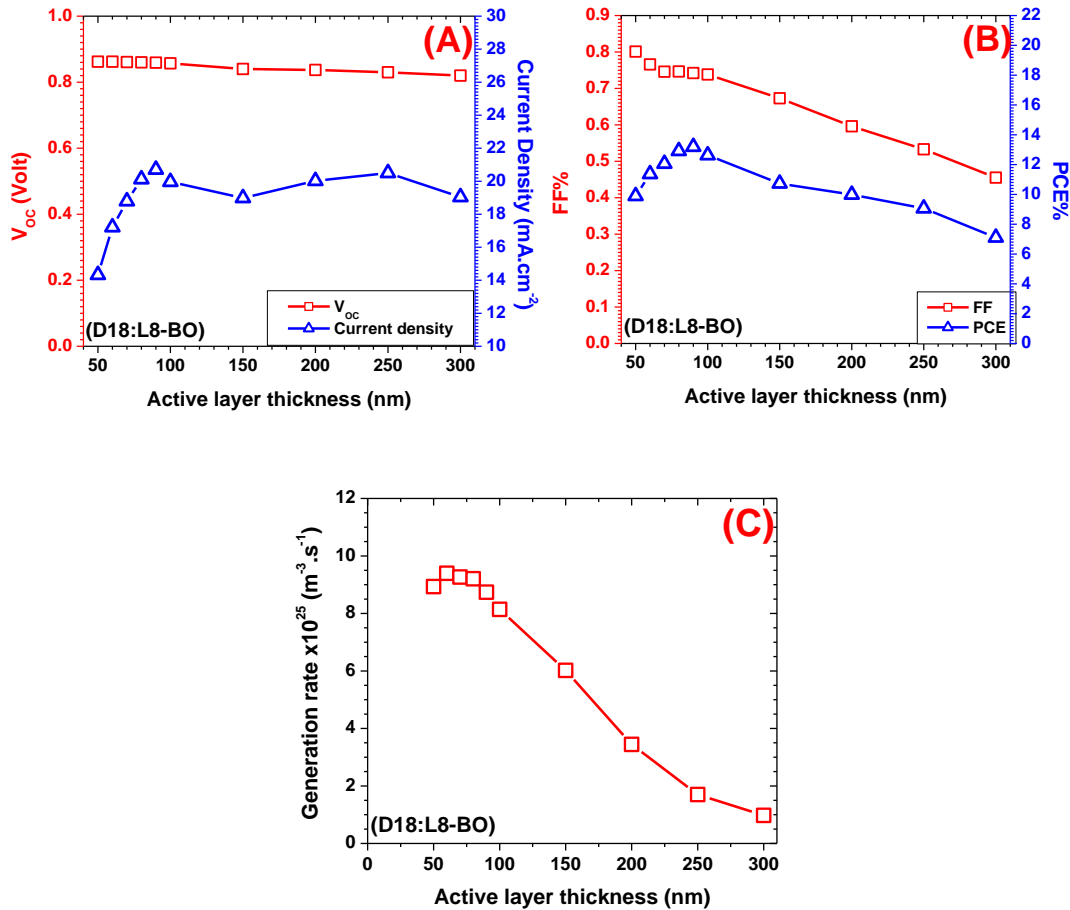

Fig 2. The solar cell parameters as a function of active layer (D18:L8-BO) thickness (A) V_{OC} and J_{SC}, (B) FF and PCE, and (C) Generation rate

The variation in OSCs performance with different active layer thickness is shown in Fig. 2A and Fig. 2B. Device with active layer thickness of 50 nm shows a PCE of 9.89% correlated to FF of 80.11%, J_{SC} of 14.33 mA.cm^{-2} and V_{OC} of 0.862 Volt. After increasing the active layer thickness to 90 nm, obvious enhancement is observed in the overall performance with increase PCE to 13.2% and J_{SC} to 20.7 mA/cm^{-2}. Upon light absorption, the light intensity inside the active layer is decreased exponentially with position inside the active layer based on Lambert-Beer theory. For a thin layer, the light passes through it and reaches the other side without decreasing much in the intensity, therefore, higher generation rate is occurred and consequently, higher current density is occurred (Islam, 2021). Fig.2C indicates a linear decrease in the generation rate with the active layer thicknesses However, at thicknesses below 100nm, the optimum thickness for better generation rate is for the thicknesses below 100nm. Thicker layers can absorb more light, but if the layer becomes too thick, recombination losses may increase, and charge

transport can become less efficient, reducing the effective generation rate (Boudia et al., 2024). The Beer-Lambert law illustrates this relationship, showing that the generation rate (G) is often proportional to the incident light intensity (I) and the absorption coefficient (α):

$$G = \alpha I (1 - e^{-\alpha d})$$

where (d) is the active layer thickness. While the generation rate initially increases with thickness due to enhanced light absorption, it may eventually level off or decline due to increased recombination and transport inefficiencies. Thus, the generation rate is positively correlated with active layer thickness up to an optimal point, beyond which it may decrease, underscoring the need for careful thickness optimization in solar cells (Boudia et al., 2024). The increase in JSC with thicker active layers is due to enhanced EQE within the 1.5 eV to 3.2 eV range (corresponding to higher photo-harvesting), PCE ultimately decreased due to a significant drop FF, caused by inefficient charge transport and increased recombination losses, which reducing the benefits of improved light absorption (Zang et al., 2018). FF is defined by the equation $FF = V_{max} J_{max} / V_{OC} J_{SC}$ 100%, where V_{max} and J_{max} is the voltage and the current density at the maximum power point on J-V curve, respectively (Al hashimi et al., 2023). When the electric field at the maximum power point ($V_{max} J_{max}$) of J-V curve is smaller than that at short-circuit condition, a lower dissociation rate and a higher recombination rate is occurred. FF decreases to 56.7% when thicker active layer is employed; this results in smaller electric field due to the larger distance between the electrodes and therefore lower FF is presented (Lee et al. 2009). To achieve high V_{OC}, high band gap donor material is desired (Hofinger et al., 2022). In here, D18 has a band gap close to 2.2 eV, this contributes in higher V_{OC}. The latter has shown no significant change in its value when the active layer thickness is increased as it is mainly defined by the difference between the $HOMO_{donor}$ and the $LUMO_{acceptor}$ (Kadem et al. 2018). Generally, PCE of OSCs are limited by two factors; carrier mobility and exciton diffusion lengths (Li et al., 2005). When diffusion length is nearly or higher than the active layer thickness, charge recombination is reduced. Hence, thinner active layer is beneficial for charge carrier extraction (El-Nahass & Abd El-Rahman, 2007). PCE as high as 13.2% is achieved when the active layer thickness is 90 nm. This thickness is considered as the optimum active layer thickness for D18:L8-BO blend as the higher active layer thicknesses larger than 90nm result in deteriorated in PCE.

2.2 PM6:L8-BO active layer

This section focuses on changing the donor material D18 by another donor material PM6 which has almost the same band gap value of D18 donor material and lower diffusion length of about 14nm compare to D18 (Zhu et al., 2022). PM6 has also similar chemical structures of D18 donor material, however, the difference in the HOMO and LUMO positions between them may affects the OSC performance; such energy level alignments might be beneficial for harvesting short and medium wavelengths' energies and forming cascade energy levels (Liu, 2021). The J-V curves of the OSCs with different PM6:L8-BO active layer thickness ranging from 50nm to 300nm is shown in Fig. 3A. The increasing in the active layer thickness enhances OSCs' performance, especially current density and PCE. As mentioned earlier, thicker active layer contributes in higher absorption characteristics as shown in Fig. 3B. The energy level alignments of PM6:L8-BO based OSCs is illustrated in Fig. 3C. The higher efficiency is attributed to better exciton dissociation, charge collection efficiency, and more balanced charge transport. Optimizing the active layer thickness requires balancing the enhancement of photon absorption with the reduction of charge recombination. Thinner layers shorten the travel distance for charge carriers, which enhances transport but may restrict the absorption range. In contrast, thicker layers can capture more light, yet they may experience lower generation rates due to increased recombination losses. Our research identified an optimal intermediate thickness that maximizes photon

absorption over a wide wavelength range while ensuring efficient charge transport, resulting in improved device performance (Boudia et al., 2024).

Further increase in the active layer thickness above 100nm results in declining the overall performance. The energy band alignment of this blend contributes in slightly higher V_{OC} of 0.86Volt compare to D18:L8-BO based OSCs. This is attributed to the higher HOMO level in PM6 (5.24 eV) compare to D18 (5.2 eV) as the V_{OC} is mainly defined by the difference between the $HOMO_{donor}$ and the $LUMO_{acceptor}$ (Kadem et al., 2018). Results in Fig.4 show that when the active layer thickness is 50 nm, a PCE of 9.41% is observed correlated to FF of 81.4%, V_{OC} of 0.858 Volt and J_{SC} of 13.47 mA.cm^{-2}.
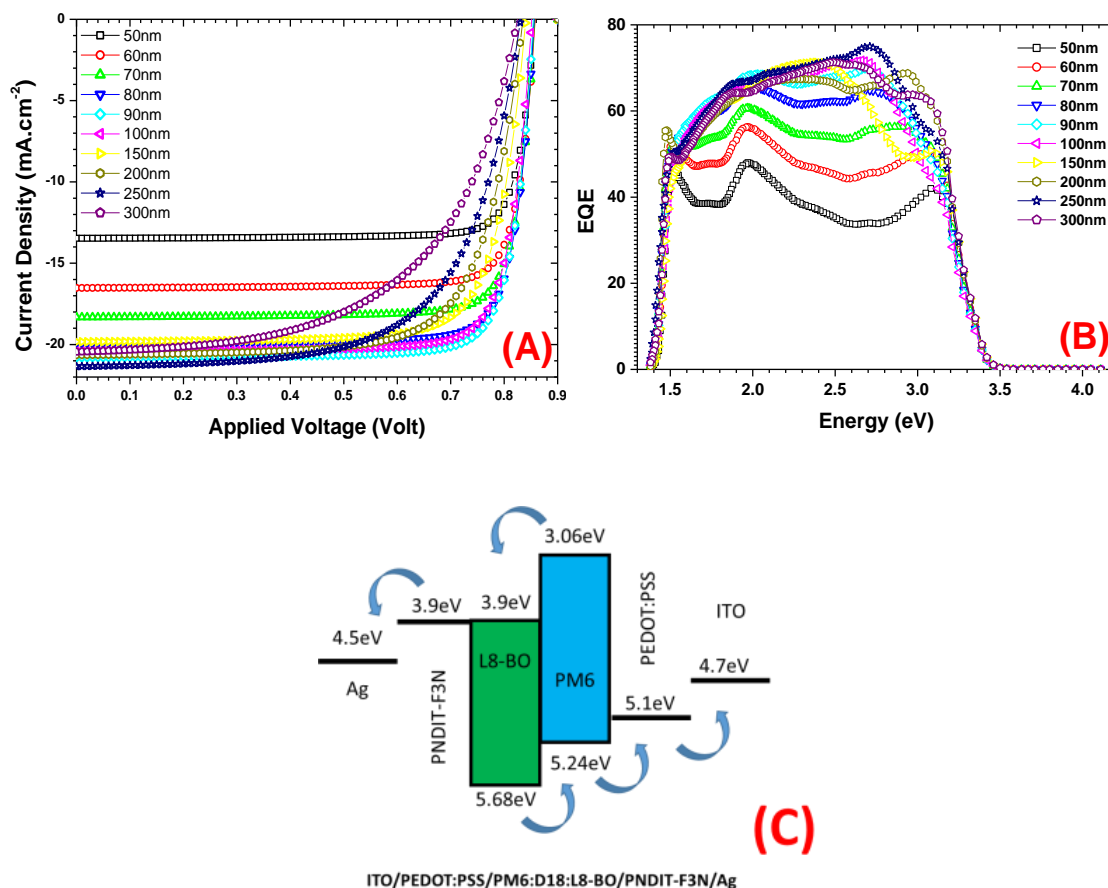

Fig 3. (A) J-V curves (B) EQE spectra and (C) Energy level alignments, of PM6:L8-BO based OSCs

Increasing active layer thickness to 90nm results in PCE of 13.52% associated with increasing J_{SC} to 20.8 mA.cm^{-2} and reducing FF to 76%, whereas V_{OC} has demonstrated similar value. The increase in the current density is ascribed to the increase in the active layer thickness which results in higher photon absorption and generation rate as shown in Fig.4B. Moreover, the higher PCE is ascribed to the higher J_{SC}. Thicker active layer (300nm) results in decreasing the overall performance where PCE reduces to 9.5%, FF to 56.7%, V_{OC} to 0.823 Volt, whereas, J_{SC} exhibited similar value. For such active layer, the optimum thickness is found to be 90nm.

2.3 PM6:D18:L8-BO active layer

To further improve the OSC performance, a ternary active layer based on PM6:D18:L8-BO active layer is examined. Fig. 5A shows the JV curve of the ternary blend based OSC and their respective EQE shown in Fig. 5B.
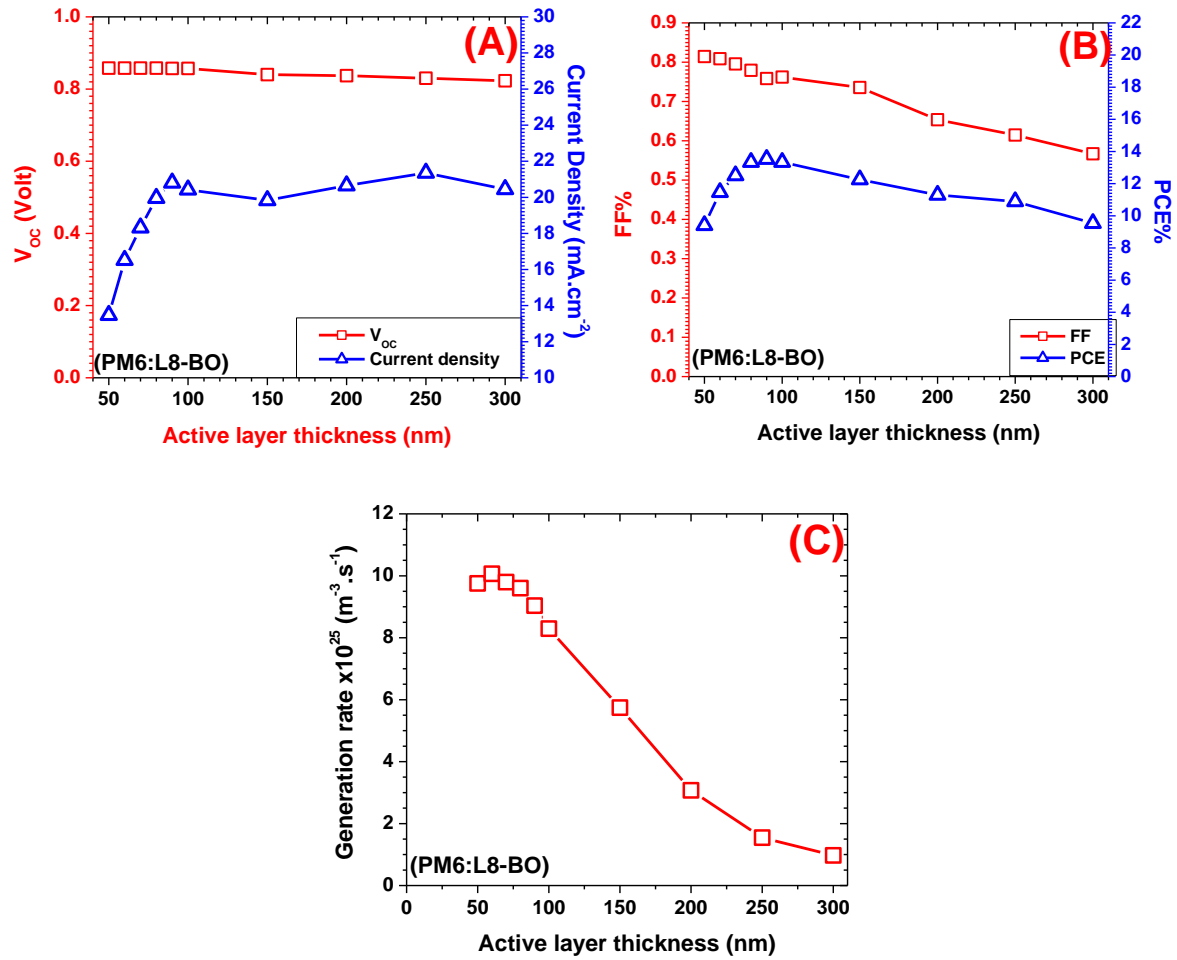
Fig 4. The solar cell parameters as a function of active layer (PM6:L8-BO) thickness (A) V_{OC} and J_{SC}, (B) FF and PCE, and (C) Generation rate

Results indicate enhancing the overall performance with increasing the active layer thickness to 90nm, further increase above 100nm results in declining the performance. The increase in the EQE spectra with increasing active layer thickness results in more charge carriers' absorption and generation (Zang et al., 2018), but the charge carriers can't reach the respective electrode due to the inefficient charge carrier transport and increase recombination loss. The photocurrent of solar cells influenced by the number of photons absorbed in the active layer. As long as the pathway for charge collection is high (thicker active layer), the chance for separated charges to recombine increases (Nam et al., 2010). The energy level cascade for the ternary blend presented in Fig. 5C plays a significant role in enhancing the exciton diffusion length and contributes in higher FF compare to the above mentioned blends (Zhu et al., 2022). Fig. 6 illustrates the OSC parameters of the ternary blend PM6:D18:L8-BO, where PCE if found to be 12.23% for the device with active layer thickness of 50nm with V_{OC} of 0.88 Volt, FF of 84.3% and J_{SC} of 16.46 mA.cm^{-2}. Increasing active layer thickness to 80 nm results in higher PCE of 17.5% with a FF of 83%, J_{SC} of 23.97 mA.cm^{-2} and V_{OC} of 0.88 Volt. The increase in the current density is attributed to the enhancement in the absorption properties as well as the enhancement in the charge carriers' diffusion length. Enhancing the diffusion length results in higher charge collection especially for an optimum active layer thickness. Zhu and co-authors proved that adding D18 to PM6:L8-BO enhances the exciton diffusion length in the donor phase (Zhu et al., 2022).
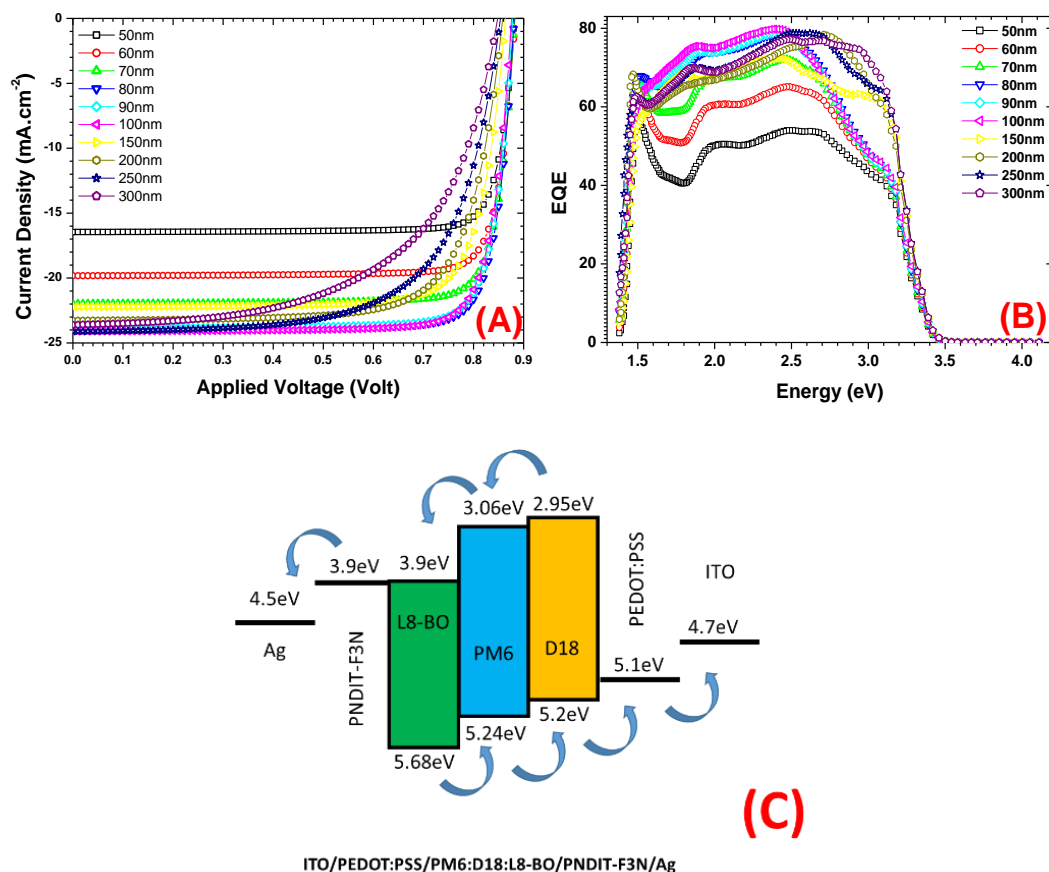
Fig 5. (A) J-V curves (B) EQE spectra and (C) Energy level alignments, of PM6:D18:L8-BO based OSCs

Further increase in the active layer thickness results in higher absorption characteristics and therefore higher charge carrier generation. However, the decline in the FF at the maximum power point indicating high recombination rate and charge loss in the device when the active layer thickness increases (Nam et al., 2010). FF of 84.34% is exhibited in the device with active layer thickness 50nm, this value decreases linearly when the active layer thickness increases to reach 57.2% at 300nm thickness, which is in good agreement with previous report (Sievers et al., 2006). The ternary blend based devices show a higher V_{OC} compared to binary blend based devices, attributed to efficient exciton dissociation and enhanced charge transport properties (Sievers et al., 2006). Additionally, the energy level alignment of the materials used (see Fig. 5C) influences V_{OC} and overall performance of the ternary blend relative to binary solar cells. The optimal active layer thickness for the ternary blend is 80 nm.

2.4 The effect of ETL thickness

The effects of the electron transport layer (ETL) thickness are evaluated in this section as it can play a significant role in the OSC performance; ETL controls the flow of electrons to their respective electrode (Vilkman et al., 2018). Interfacial layers, usually enhances the charge extraction by facilitating the energy levels alignment and produces appropriate charge transport pathways (Lee et al., 2023). Using different ETL thickness is essential to control the electron flow to the electrode by enhancing the interfacial properties. It has been proved that using ultra-thin ETL supports a good interfacial contact by reducing the interfacial traps between the cathode and active layer (Chi et al., 2017). The conjugated polymer PNDIT-F3N was employed as the cathode interlayer because it has good interface properties (Dong et al., 2019).
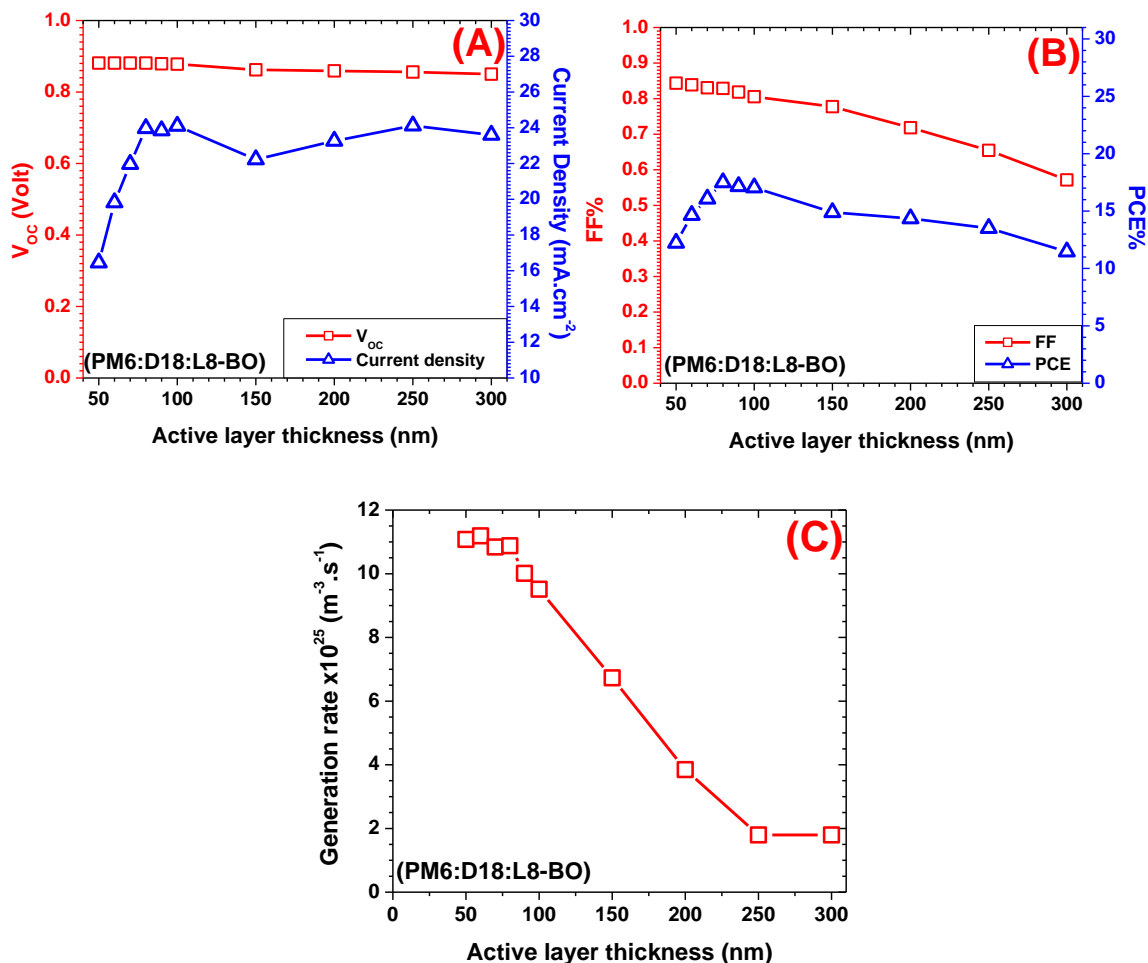
Fig 6. The solar cell parameters as a function of active layer (PM6:D18:L8-BO) thickness (A) V_{OC} and J_{SC}, (B) FF and PCE, and (C) Generation rate

Different thicknesses of PNDIT-F3N as ETL is used (10nm, 15nm, 20nm, 25nm); the devices are evaluated using the optimum active layer thicknesses of the ternary blend PM6:D18:L8-BO active layer. Biswas et al., 2023 studied the impact of ETL thickness on the P3HT:ICBA-based OSCs. They achieved a PCE of 5.0% by using 2.2 nm thick ETL. Nithya et al. (2020) reported that increasing the ETL thickness results in a slight increase in V_{OC} and J_{SC}, while a slight decrease in FF value is reported. The device structure used in this section is as follow: ITO/PEDOT:PSS (200nm)/PM6:D18:L8-BO (80nm)/ETL (different thicknesses)/Ag. Fig. 7A show the J-V characteristics of the ternary blend based devices with different ETL thicknesses. Results indicates an enhancement in the device performance when the ETL thickness is 20nm compare to device with ETL thickness of 10nm. The PCE is increased to achieve as high as 19.5% (ETL thickness is 20nm) compare to 17.5% (ETL thickness is 10nm). This is associated to increase to J_{SC} of 26.8 mA.cm^{-2} (ETL thickness is 20nm) compare to 23.97 mA.cm^{-2} (ETL thickness is 10nm). While FF and V_{OC} has demonstrated no change in their values. The decrease in J_{SC} when the ETL thickness is 25nm to 20.92 mA.cm^{-2} is correlated with a decrease in PCE to 15.2%. Such decrease is might be due to the reduction in the shunt resistance of the device when the ETL is thicker. This might have interrupted the exciton dissociation and therefore higher charge carrier recombination occurred (Chi et al., 2017).
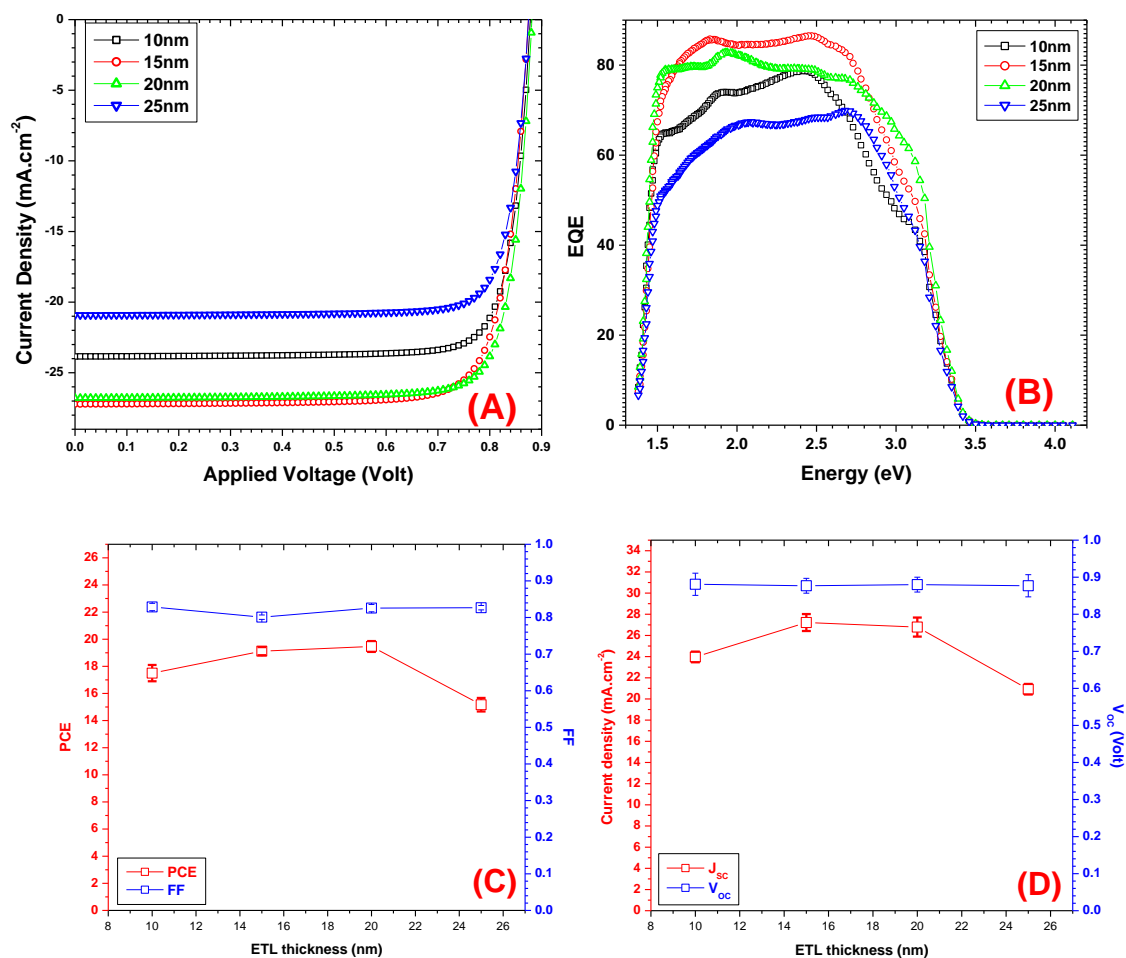
Fig 7. (A) J-V curves (B) EQE spectra, (C) FF and PCE, and (D) V_{OC} and J_{SC}, of the PM6:D18:L8-BO based OSCs with different ETL thicknesses

3. CONCLUSION

Two approaches are evaluated in the current study: firstly, the effects of active layer and the electron transport layer thicknesses, and secondly, the use of non-fullerene donor and acceptor materials to fabricate binary and ternary organic solar cells. Results indicated that for D18:L8-Bo and Pm6:L8-BO active layer based solar cells that the optimum active layer thickness is 90nm with PCE of 13.2% and 13.52%, respectively. This was attributed to the enhancement in the current density. The ternary blend solar cell based on PM6:D18:L8-BO active layer has shown an enhancement in the PCE to reach as high as 17.5% in the optimum active layer thickness of 80nm. this device is further enhanced when using electron transport layer thickness of 20nm with a PCE of 19.5%. Such enhancement is attributed to the enhancement in the interface properties.

NOMENCLATURE

OSCs	Organic solar cells	HOMO	Highest occupied molecular orbital
PCE	Power conversion efficiency	LUMO	Lowest unoccupied molecular orbital
V_{OC}	Open Circuit Voltage		

| D18 | Poly[(2,6-(4,8-bis(5-(2-ethylhexyl-3-fluoro) thiophen-2-yl)- benzo [1,2-b:4,5-b'] dithiophene)) -alt-5,5'- (5,8-bis(4-(2-butyloctyl) thiophen-2-yl) dithieno [3',2':3,4;2",3":5,6] benzo[1,2-c][1,2,5]thiadiazole)] | L8-BO | (2,2'- ((2Z,2'Z)- ((3,9-bis (2-butyloctyl) -12, 13-bis (2-ethylhexyl) -12,13-dihydro -[1,2,5]thiadiazolo[3,4-e]thieno[2″,3″:4′,5′] hieno [2′,3′:4,5] pyrrolo [3,2-g] thieno [2′,3′:4,5] thieno [3,2-b] indole-2,10-diyl) bis (methaneylylidene)) bis(5,6-difluoro-3-oxo-2,3-dihydro-1H-indene-2,1-diylidene))dimalononitrile) |
| PM6 | Poly[(2,6-(4,8-bis(5-(2-ethylhexyl-3-fluoro) thiophen-2-yl) -benzo [1,2-b:4,5-b'] dithiophene))-alt- (5,5-(1',3'-di-2-thienyl-5', 7' -bis (2-ethylhexyl) benzo [1',2'-c:4',5'-c']dithiophene-4,8-dione)] | | |

REFERENCES

Al Hashimi, M.K., AL-Mosawi, B.T. and Kadem, B.Y. (2023). The Effects of Solvent Treated PEDOT: PSS Layer to Enhance Polymer Solar Cells Efficiency. *Journal of Nanostructures*, 13(1):122-131.

Bishnoi, S., Datt, R., Arya, S., Gupta, S., Gupta, R., Tsoi, W.C., Sharma, S.N., Patole, S.P. and Gupta, V. (2022). Engineered cathode buffer layers for highly efficient organic solar cells: a review. *Advanced Materials Interfaces*, 9(19):2101693.

Biswas, S., Lee, Y., Choi, H. and Kim, H. (2023). Recent developments in non-fullerene-acceptor-based indoor organic solar cells. *Journal of Physics: Materials*, 6(4):042002.

Boudia, M.E.A., Wang, Q. and Zhao, C. (2024). Optimization of the Active Layer Thickness for Inverted Ternary Organic Solar Cells Achieves 20% Efficiency with Simulation. Sustainability, 16(14), p.6159.

Chi, D., Huang, S., Yue, S., Liu, K., Lu, S., Wang, Z., Qu, S. and Wang, Z. (2017). Ultra-thin ZnO film as an electron transport layer for realizing the high efficiency of organic solar cells. *RSC advances*, 7(24):14694-14700.

Dong, S., Zhang, K., Jia, T., Zhong, W., Wang, X., Huang, F. and Cao, Y. (2019). Suppressing the excessive aggregation of nonfullerene acceptor in blade-coated active layer by using n-type polymer additive to achieve large-area printed organic solar cells with efficiency over 15%. *EcoMat*, 1(1):12006.

El-Nahass, M.M. and Abd El-Rahman, K.F. (2007). Investigation of electrical conductivity in Schottky-barrier devices based on nickel phthalocyanine thin films. *Journal of alloys and compounds*, 430(1-2):194-199.

Gao, Y., MacKenzie, R.C.I., Liu, Y., Xu, B., van Loosdrecht, P. H. M. and Tian, W. (2015), Engineering Ultra Long Charge Carrier Lifetimes in Organic Electronic Devices at Room Temperature, *Adv. Mater. Interfaces*, 2:1400555.

Hassan, A., Kadem, B. and Cranton, W. (2017). Organic solar cells: Study of combined effects of active layer nanostructure and electron and hole transport layers. *Thin Solid Films*, 636:760-764.

He, C., Pan, Y., Ouyang, Y., Shen, Q., Gao, Y., Yan, K., Fang, J., Chen, Y., Ma, C.Q., Min, J. and Zhang, C. (2022). Manipulating the D: A interfacial energetics and intermolecular packing for 19.2% efficiency organic photovoltaics. *Energy & Environmental Science*, 15(6):2537-2544.

Heeger, A.J. (2014). 25th anniversary article: bulk heterojunction solar cells: understanding the mechanism of operation. *Advanced materials*, 26(1):10-28.

Hofinger, J., Weber, S., Mayr, F., Jodlbauer, A., Reinfelds, M., Rath, T., Trimmel, G. and Scharber, M.C. (2022). Wide-bandgap organic solar cells with a novel perylene-based non-fullerene acceptor enabling open-circuit voltages beyond 1.4 V. *Journal of Materials Chemistry A*, 10(6):2888-2906.

Islam, M.S. (2021). Investigation of the Current of P3HT: PCBM-Based Organic Solar Cell Extracting the Spatial Recombination Coefficient of the Active Layer. *IEEE Access*, 9:130502-130518.

Kadem, B., Cranton, W. and Hassan, A. (2015). Metal salt modified PEDOT: PSS as anode buffer layer and its effect on power conversion efficiency of organic solar cells. *Organic Electronics*, 24:73-79.

Kadem, B., Hassan, A. and Cranton, W. (2016). Efficient P3HT: PCBM bulk heterojunction organic solar cells; effect of post deposition thermal treatment. *Journal of Materials Science: Materials in Electronics*, 27:7038-7048.

Kadem, B., Kaya, E.N., Hassan, A., Durmuş, M. and Basova, T. (2019). Composite materials of P3HT: PCBM with pyrene substituted zinc (II) phthalocyanines: Characterisation and application in organic solar cells. *Solar Energy*, 189:1-7.

Kadem, B.Y., Kadhim, R.G. and Banimuslem, H. (2018). Efficient P3HT: SWCNTs hybrids as hole transport layer in P3HT: PCBM organic solar cells. *Journal of Materials Science: Materials in Electronics*, 29(11):9418-9426.

Lee, H.W., Biswas, S., Lee, Y. and Kim, H. (2023). Over 23% Efficiency under Indoor Light in Gallium-Doped Zinc Oxide Electron Transport Layer-based Inverted Organic Solar Cell to Power IoT Devices. *IEEE Internet of Things Journal.* 10(8): 15923 − 15930.

Lee, J.U., Cirpan, A., Emrick, T., Russell, T.P., Jo, W.H. (2009). Synthesis and photophysical property of well-defined donor–acceptor diblock copolymer based on regioregular poly(3-hexylthiophene) and fullerene, *J. Mater. Chem.* 19:1483–1489.

Lee, M.H. (2020). Performance and matching band structure analysis of tandem organic solar cells using machine learning approaches. *Energy Technology*, 8(3):1900974.

Li, G., Shrotriya, V., Yao, Y. and Yang, Y. (2005). Investigation of annealing effects and film thickness dependence of polymer solar cells based on poly (3-hexylthiophene). *Journal of Applied Physics*, 98(4):043704.

Liu, Z. (2021). Enhancing the photovoltaic performance with two similar structure polymers as donors by broadening the absorption spectrum and optimizing the molecular arrangement. *Organic Electronics*, 93:106153.

MacKenzie, R.C.I., Balderrama, V. S., Schmeisser, S., Stoof, R., Greedy, S., Pallarès, J., Marsal, L. F., Chanaewa, A., von Hauff, E. (2016), Loss mechanisms in high efficiency polymer solar cells, *Advanced Energy Materials*, 6(4):1501742.

Nam, Y.M., Huh, J. and Jo, W.H. (2010). Optimization of thickness and morphology of active layer for high performance of bulk-heterojunction organic solar cells. *Solar Energy Materials and Solar Cells*, 94(6):1118-1124.

Nithya, K.S. and Sudheer, K.S. (2020). Numerical modelling of non-fullerene organic solar cell with high dielectric constant ITIC-OE acceptor. *Journal of Physics Communications*, 4(2):025012.

Sharma, V. V., Landep, A., Lee, S. Y., Park, S. J., Kim, Y. H., & Kim, G. H. (2023). Recent advances in polymeric and small molecule donor materials for Y6 based organic solar cells. *Next Energy*, 2:100086.

Sievers, D.W., Shrotriya, V., Yang, Y. (2006). Modeling optical effects and thickness dependent current in polymer bulk-heterojunction solar cells, *J. Appl. Phys.* 100:114509-1–114509-7.

Tokmoldin, N., Vollbrecht, J., Hosseini, S.M., Sun, B., Perdigón-Toro, L., Woo, H.Y., Zou, Y., Neher, D. and Shoaee, S., (2021), Explaining the fill-factor and photocurrent losses of nonfullerene acceptor-based solar cells by probing the long-range charge carrier diffusion and drift lengths. *Advanced Energy Materials*, 11(22):2100804.

Vilkman, M., Väisänen, K.L., Apilo, P., Po, R., Välimäki, M., Ylikunnari, M., Bernardi, A., Pernu, T., Corso, G., Seitsonen, J. and Heinilehto, S., (2018) Effect of the electron transport layer on the interfacial energy barriers and lifetime of R2R printed organic solar cell modules. *ACS Applied Energy Materials*, 1(11):5977-5985.

Xue, R., Zhang, J., Li, Y. and Li, Y., (2018), Organic solar cell materials toward commercialization. *Small*, 14(41):1801793.

Yuan, J., Zhang, Y., Zhou, L., Zhang, G., Yip, H.L., Lau, T.K., Lu, X., Zhu, C., Peng, H., Johnson, P.A., Leclerc, M., Yong Cao, Ulanski, J., Li, Y., Zou. Y. (2019). Single-Junction Organic Solar Cell with over 15% Efficiency Using Fused-Ring Acceptor with Electron-Deficient Core, *Joule*, 3(4):1140-1151.

Yuan, J., Zhang, Y., Zhou, L., Zhang, G., Yip, H.L., Lau, T.K., Lu, X., Zhu, C., Peng, H., Johnson, P.A. and Leclerc, M. (2019). Single-junction organic solar cell with over 15% efficiency using fused-ring acceptor with electron-deficient core. *Joule*, 3(4):1140-1151.

Zang, Y., Xin, Q., Zhao, J. and Lin, J. (2018). Effect of active layer thickness on the performance of polymer solar cells based on a highly efficient donor material of PTB7-Th. *The Journal of Physical Chemistry C*, 122(29):16532-16539.

Zheng, Z., Wang, J., Bi, P., Ren, J., Wang, Y., Yang, Y., Liu, X., Zhang, S. and Hou, J. (2022). Tandem organic solar cell with 20.2% efficiency. *Joule*, 6(1):171-184.

Zhu, L., Zhang, M., Xu, J., Li, C., Yan, J., Zhou, G., Zhong, W., Hao, T., Song, J., Xue, X. and Zhou, Z. (2022). Single-junction organic solar cells with over 19% efficiency enabled by a refined double-fibril network morphology. *Nature Materials*, 21(6):656-663.